Porous Organic Polymers Containing Active Metal Centers for Suzuki-Miyaura Heterocoupling Reactions

Noelia Esteban[1], María L. Ferrer[2], Conchi O. Ania[3], José G. de la Campa[4], Ángel E. Lozano[1,4,5], Cristina Álvarez[4,5,]*, Jesús A. Miguel[1,]*

1. IU CINQUIMA, Universidad de Valladolid, Paseo Belén 5, E-47011 Valladolid, Spain.

2. Materials Science Factory, Instituto de Ciencia de Materiales de Madrid, ICMM-CSIC, Campus de Cantoblanco, 28049 Madrid, Spain.

3. CEMHTI CNRS (UPR 3079), University of Orléans, 45071 Orléans, France.

4. Department of Applied Macromolecular Chemistry, Instituto de Ciencia y Tecnología de Polímeros, ICTP-CSIC, Juan de la Cierva 3, E-28006 Madrid, Spain.

5. SMAP, UA-UVA_CSIC, Associated Research Unit to CSIC. Universidad de Valladolid, Facultad de Ciencias, Paseo Belén 7, E-47011 Valladolid, Spain.

ABSTRACT

A new generation of confined palladium(II) catalysts covalently attached inside of porous organic polymers (POPs) has been attained. The synthetic approach employed was straightforward, and no prerequisite of making any modification of the precursor polymer was needed. First off, POP-based catalytic supports were obtained by reacting one symmetric trifunctional aromatic monomer (1,3,5-triphenylbenzene) with two ketones having electron-withdrawing groups (4,5-diazafluoren-9-one, DAFO, and isatin) in superacidic media. The homopolymers and copolymers were made using stoichiometric ratios between the functional groups and they were obtained with quantitative yields after an optimization of reaction conditions. Moreover, the number of chelating groups (bipyridine moieties) available to bind Pd(II) ions in the catalyst supports was modified using different DAFO/isatin ratios. The resulting amorphous polymers and copolymers showed high thermal stability, above 500 ºC, and moderate-high specific surface areas (from 760 to 935 m^2g^{-1}), with high microporosity contribution (from 64% to 77%). Next, POP-supported Pd(II) catalyst were obtained by simple immersion of the catalyst supports in a palladium(II) acetate solution, observing that the metal content was similar to that theoretically expected according to the amount of the bipyridine groups. The catalytic activity of these heterogeneous catalysts was explored for the synthesis of biphenyl and terphenyl compounds, via the Suzuki-Miyaura cross-coupling reaction using a green solvent (ethanol/water), low palladium loads and aerobic conditions. The findings showed excellent catalytic activity with quantitative product yields. Additionally, the recyclability of the catalysts, by simply washing it with ethanol, was excellent, with a sp^2-sp^2 coupling yield higher than 95% after 5 cycles of use. Finally, the feasibility of these catalysts to be employed in tangible organic reactions was assessed. Thus, the synthesis of a bulky compound,

4-4″-dimethoxy-5'-*tert*-butyl-m-terphenylene, which is a precursor of a thermally rearrangement monomer, was scaled-up to 2 g, with high conversion and 96% yield of pure product.

INTRODUCTION

Suzuki-Miyaura cross-coupling reaction between haloderivatives and boronic acids catalyzed by Pd(0) compounds, which was awarded with the Nobel Laureate in 2010,[1,2] is one of the most reliable, efficient and practical methodologies for the formation of C-C bonds since its first reports in 1979.[2–6] In particular, the reaction is a versatile and powerful methodology, for example, in the construction of biaryl compounds and the substitution and modification of aromatic and heteroaromatic moieties.[6–8] In this context, the Suzuki-Miyaura reaction is used in many research fields because it permits the efficient discovery, development and synthesis of pharmaceutical and chemical compounds, of different kinds of engineering materials (liquid crystals, polymers, molecular wires, etc.), coordination chemistry materials, supramolecular chemistry, and diverse functional materials.[1,8–12]

Nowadays, one of the main concerns in scientific research, especially for pharmaceutical and chemical industries, is the search for greener, safer, environmentally friendly and efficient technologies.[13–16] Specifically, the use of recyclable heterogeneous catalysts for organic synthesis allows for the reduction of waste production and the optimization of the efficiency of the synthetic process, and therefore research in this area is of utmost importance.

The inclusion of metal catalysts confined in microporous cavities has given rise to materials having high turnover number, TON, and turnover frequency, TOF, high chemical regioselectivities, high recyclability and low metal contamination of the obtained products.[12,17–23] It has been demonstrated that catalyst confinement produces a variation in the energetic and kinetic properties of the catalytic process, which improves its yield and selectivity.[24]

Porous organic polymers, POPs, have shown great efficiency as new catalyst supports in heterogeneous catalysis, thanks to their high surface area and structural stability, designable porosity, controllable intrinsic functional groups and the possibility of incorporating high catalyst loads.[13,14,25–27] Likewise, numerous reports on POP-immobilized palladium catalysts have shown their suitability for green Suzuki-Miyaura coupling reactions.[28–30] Thus, Du et al.[28] synthesized heterogeneous catalysts, Pd/Cy-pips, by immobilizing Pd(II) onto a nitrogen-rich heptazine-based porous frameworks. The Pd/Cy-pips showed efficient catalytic performance for the reaction of a variety of activated aryl bromides with phenylboronic acid in EtOH/water at 40 ºC and 1 h. Qian et al.[29] reported thiadiazole-containing heterogeneous catalysts, Pd@DTE in EtOH/water at 50 ºC employing large reaction times (6-20 h), which showed good catalytic activity in coupling hetero halides and sterically hindered aryl halides with phenylboronic acid. Xu et al.[30] synthesized palladium immobilized catalysts on 1,10-phenanthroline-containing microporours porous polymers, MOP-Pds, which can efficiently catalyze the Suzuki coupling reaction in EtOH/H_2O at 80 ºC with reaction times ranging from 1 h to 3 h. All of these catalysts could be reused for several times without a significant loss of its catalytic activity.

The development of new POP materials with high thermal stability and high specific surface area is booming for advanced applications such as CO_2 capture, gas separation and storage, sensor preparation or heterogeneous catalysts.[31–36] These POP materials can be manufactured using a variety of different methodologies to achieve tailored properties. Olah et al. proposed the activation of electrophiles in Brønsted or Lewis super acidic media in order to obtain reactants that show a significantly higher electrophilic character.[37–40] Following Olah's methodology, Zolotukhin et al. obtained linear polymers by using a one-pot S_EAr reaction of ketones having electron-withdrawing groups (for instance, isatin or trifluoroacetophenone) with diaromatic hydrocarbons (for instance,

biphenyl or p-terphenyl). These linear polymers showed high molecular weight and exhibited good chemical and thermal stability (around 500 ºC). Furthermore, they could be employed as gas separation membranes, which showed excellent values of permeability and selectivity.[41–44]

Recently, in our research group, a new generation of porous polymer network were synthesized following Olah's methodology, by reaction of ketones having electron-withdrawing groups (i.e.; isatin and trifluoroacetophenone) with rigid trifunctional aromatic monomers (triptycene and 1,3,5-triphenylbenzene) employing triflic acid as a superacidic media.[45] These polymers showed high surface areas between 580 and 790 m^2 g^{-1}, high thermal stability and excellent CO_2 uptakes and were employed as fillers to prepare mixed matrix membranes displaying excellent gas separation performances.[36]

Following this research line, we have now introduced a set of microporous polymer networks, POPs, having a rigid bipyridine moiety in its structure. These POPs were able to efficiently form confined Pd catalysts by simple immersion in a Pd(II) acetate solution. The catalysts thus obtained have been evaluated for the Suzuki-Miyaura reaction of a wide variety of haloaromatic derivatives and boronic acids.

2. EXPERIMENTAL PART

2.1. Materials

All reagents were purchased and used without any purification except 4,5-diazafluoren-9-one (DAFO), which was synthesized in our laboratory following the methodology described elsewhere.[46,47] The detailed synthesis of DAFO is described in the Supporting Information (SI).

2.2. Techniques

Fourier Transform Infrared (FTIR-ATR) spectra were recorded on a PerkinElmer Spectrum RX-I FT-IR spectrometer, equipped with an attenuated total reflection accessory (ATR) Pike Gladi ATR-210. Solid-state ^{13}C cross-polarization magic angle spinning NMR spectra (CP/MAS ^{13}C NMR) spectra were recorded on a Bruker Avance TM 400WB spectrometer, equipped with a 89 nm wide-bore and a 9.4 T superconducting magnet, operating at frequency of 100.6 MHz, using 1 ms contact pulses, a delay time of 3 s and a rotation rate of 11 kHz. Dynamic thermogravimetric analysis (TGA) were performed on a TA-Q500 instrument under a continuous nitrogen flow (60 mL min^{-1}), operating with a Hi-Res method at a heating rate of 20 °C min^{-1} and sensitivity and resolution parameters of 1 and 4, respectively. Wide-Angle X-Ray Scattering (WAXS) patterns were recorded in reflection mode at room temperature, using a Bruker D8 Advance diffractometer provided with a Goebel Mirror and a PSD Vantec detector. A step-scanning mode was employed for the detector, with a 2θ step of 0.024°, at a rate of 0.5 s per step. CuK$_\alpha$ (wavelength λ = 1.54 Å) radiation was used. Scanning Electron Microscopy (SEM) images were taken with a QUANTA 200 FEG ESEM on Au- metallized samples operating at an acceleration voltage of 1.5 kV in high vacuum and using the detection of secondary electrons method. Scanning electron microscopy–energy dispersive X-ray spectroscopy (SEM–EDX), used to determine the distribution of Pd in the porous polymer catalysts (Pd@POPs), was carried out by using a Scanning Electron Microscope ESEM (QUANTA 200 FEG) equipped with EDAX Genesis. XPS measurements were carried out in a SPECS (Germany) device using a Phoibos 100 hemispherical electron energy analyzer and a 5 channel multi-channeltron detector. The beam source was a non-monochromatic Mg K-α with voltage of 12.5 KV and power of 100 W. The analysis conditions were; high resolution spectra with 10 eV step energy with points acquired every 0.1 eV with a dwell time of 0.5 s. The sample was prepared as follows; the powder sample was placed and stuck on a double-sided carbon sticker

and introduced into the XPS sample holder. XPS spectra were not accumulated for long time (in order to obtain better signal/noise ratios), because Pd tends to change the oxidation state by the effect of the measurement itself. N_2 adsorption-desorption isotherms were measured at -196 °C in a volumetric analyzer (3Flex, Micromeritics), in the relative pressure range (P/P$_0$) from 10^{-5} to 1 bar. Previously, samples were degassed under vacuum at 250 °C for 10 h to remove humidity, adsorbed gases and solvent from the samples. The adsorption isotherms were used to determine the specific surface area (S$_{BET}$) by applying the Brunauer-Emmet-Teller equation, the micropore volume (V$_{micro}$) using the Dubinin-Radushkevich (DR) equation, and the total pore volume (V$_{total}$) from the amount adsorbed at 0.99 relative pressure. Pore size distributions (PSD) were evaluated using the 2D-NLDFT-HS model.[48] Each isotherm was recorded in duplicate on fresh sample aliquots, to guarantee the reproducibility (error was below 5%). The skeletal density of the samples was measured by helium picnometry in an Accupyc 1340 apparatus. The palladium content in the porous polymer catalysts was determined using a radial simultaneous ICP-OES Varian 725-Es device.

2.3. Synthesis of porous organic polymers

The methodology of formation of POPs was based on a reaction described recently.[45] Here, moreover, two reaction temperatures (room temperature and 60 ºC) and the use or not of chloroform, as a co-solvent, were tested. The 135TPB was combined with DAFO, isatin or a mixture of these monomers in molar DAFO/isatin ratios of 1/1 and 1/3.

As an example, the synthesis of 135TPB–DAFO-Isatin (4:3:3) polymer network at 60 ºC and using chloroform as co-solvent is described as follows:

An oven-dried three-necked Schlenk flask, 500 mL, equipped with a mechanical stirred and nitrogen inlet and outlet was charged with 1,3,5-triphenylbenzene, 135TPB, (2.24 g, 7.32 mmol),

isatin (0.81 g, 5.49 mmol) and DAFO (1.00 g, 5.49 mmol). Anhydrous chloroform (15 mL) was added and monomers mixture was stirred at room temperature under a nitrogen blanket. The mixture was stirred and cooled at 0 ºC, and then chilled TFSA (30 mL) was added dropwise with an addition funnel for 30-60 min. After the TFSA addition, the mixture was left to warm up to room temperature and maintained with mechanical stirring for 24 h. Subsequently, the mixture was warmed to 60 ºC and maintained for 96 h. Finally, the reaction mixture was poured onto cool distilled water, neutralized by adding a concentrated $NaHCO_3$ solution, filtered and consecutively washed with warm distilled water, methanol, acetone and chloroform. After filtering, the powder was dried at 180 ºC and 60 mbar during 24 h. The material was obtained as a brown powder in quantitative yield (99%).

2.4. Synthesis of supported Pd(II) catalysts

As an example, the synthesis of 135TPB-DAFO-Isatin (4:3:3) coordinated with palladium(II) acetate is described below:

A 25 mL oven-dried Schlenk flask, with nitrogen inlet and outlet was charged with 135TPB-DAFO-Isatin (4:3:3) (0.75 g, 1.07 mmol of DAFO groups) and 10 mL dichloromethane. The mixture was dispersed with an Ultra-turrax disperser at 6000 rpm, then palladium acetate (0.24 g, 1.07 mmol) was added and, finally, the mixture was stirred in the dark for 72 h. The product was filtered and washed with dichloromethane and acetone. After drying it at 60 °C for 16 h under 60 mbar vacuum, the material was obtained as a brown powder in 99% yield.

2.5. General procedure for the Suzuki – Miyaura cross-coupling reaction

Aryl halide (0.50 mmol), arylboronic acid (0.75-0.60 mmol), inorganic base (1 mmol) and supported Pd(II) catalyst (0.5-1% mol Pd) were added along with 5 mL of solvent (EtOH/water

(2:3)) in a 25 mL two-necked round bottom flask and heated at 80 ºC. The mixture was stirred by an ultrasonic probe under air. After the reaction was completed (between 0.5 and 2 h depending on the reactants), the mixture was extracted with dichloromethane, dried in a rotary evaporator and the conversion was evaluated by ^{1}H-NMR.

2.6. Catalyst recycling of Suzuki-Miyaura cross-coupling reactions

Recycling tests were made up as follows:

For the first cycle, aryl halide (0.50 mmol), boronic acid (0.60 mmol), Na$_2$CO$_3$ (1 mmol), POP-supported Pd(II) catalyst (0.5-4% mol) and 5 mL of solvent (EtOH/water (2:3)) were added to a flask, and the mixture was reacting with ultrasonic or magnetic stirring for 1 h at 80 ºC. Next, the mixture reaction along with 3 mL of EtOH was poured into a conical centrifuge tube and centrifuged at 4000 rpm for 5 min. The floating liquid was decanted and poured into a decantation funnel. The supported Pd(II) catalyst was centrifuged two more times with fresh EtOH and the floating liquid was also added to the decantation funnel. Then, the cross-coupling product was extracted in dichloromethane, the solvent was removed by rotatory evaporation and the final solid was characterized by ^{1}H-NMR to determine the conversion of the reaction.

For the following cycles, the same quantity of reactants with the recovered catalyst, which was taken from the centrifuge tube with the solvent, were added to the flask. The same procedure followed in the first cycle was consecutively carried out a certain number of times.

3. RESULTS AND DISCUSSION

3.1. Optimization of reaction conditions

The synthesis of POPs was achieved by reacting of a rigid trifunctional aromatic nucleophilic monomer having a D$_{3h}$ symmetry (135TPB) with ketones having electron-withdrawing groups

(DAFO, isatin or a mixture of these monomers in specific molar ratios) under superacid conditions employing TFSA as the acid promoter. The polymerization reaction occurs when the strong acid protonates the electron deficient ketone, and reacts with an aromatic nucleophile. In order to form a highly crosslinked network, a stoichiometric ratio of trifunctional monomer to bifunctional monomer (or mixed of bifunctional monomers in different molar ratios) was employed. With the target of controlling the amount of metallic catalyst in the POPs, a set of copolymers were attained by combining DAFO with isatin in molar DAFO/isatin ratios of 1/1 and 1/3. The structure of the materials and the acronyms used to refer to them are shown in Scheme 1. For comparative purposes, the homopolymer from 135TPB and isatin was also obtained using the reaction conditions previously reported.[45]

The synthesis of these POPs was optimized on varying reactions conditions, such as reaction temperature (room temperature, RT, or 60 ºC) and use or not of a co-solvent (chloroform). Table S1 summarize the reaction conditions tested in the synthesis of POPs along with the reaction yields. According to the findings, the reaction yield of all the POPs were high (> 90%), except for that of POP3 prepared at 60 ºC in TFSA. Particularly, the POPs were obtained in almost quantitative yields (99%) when a TFSA/CHCl$_3$ mixture was employed. However, in those with a higher content of DAFO, POP1 and POP2, it was necessary to hold the reaction temperature at 60 ºC for 96 h. All the POPs prepared were characterized by FTIR-ATR and CP/MAS ^{13}C-NMR (Figures S3-S10). Comparing the spectra, it was observed that the chemical structure of POP1 and POP2, having higher percentage of DAFO, were strongly depended on temperature and reaction medium.

Scheme 1. Chemical structures of POPs. The numbers next to the monomers indicate the moles employed in the reaction.
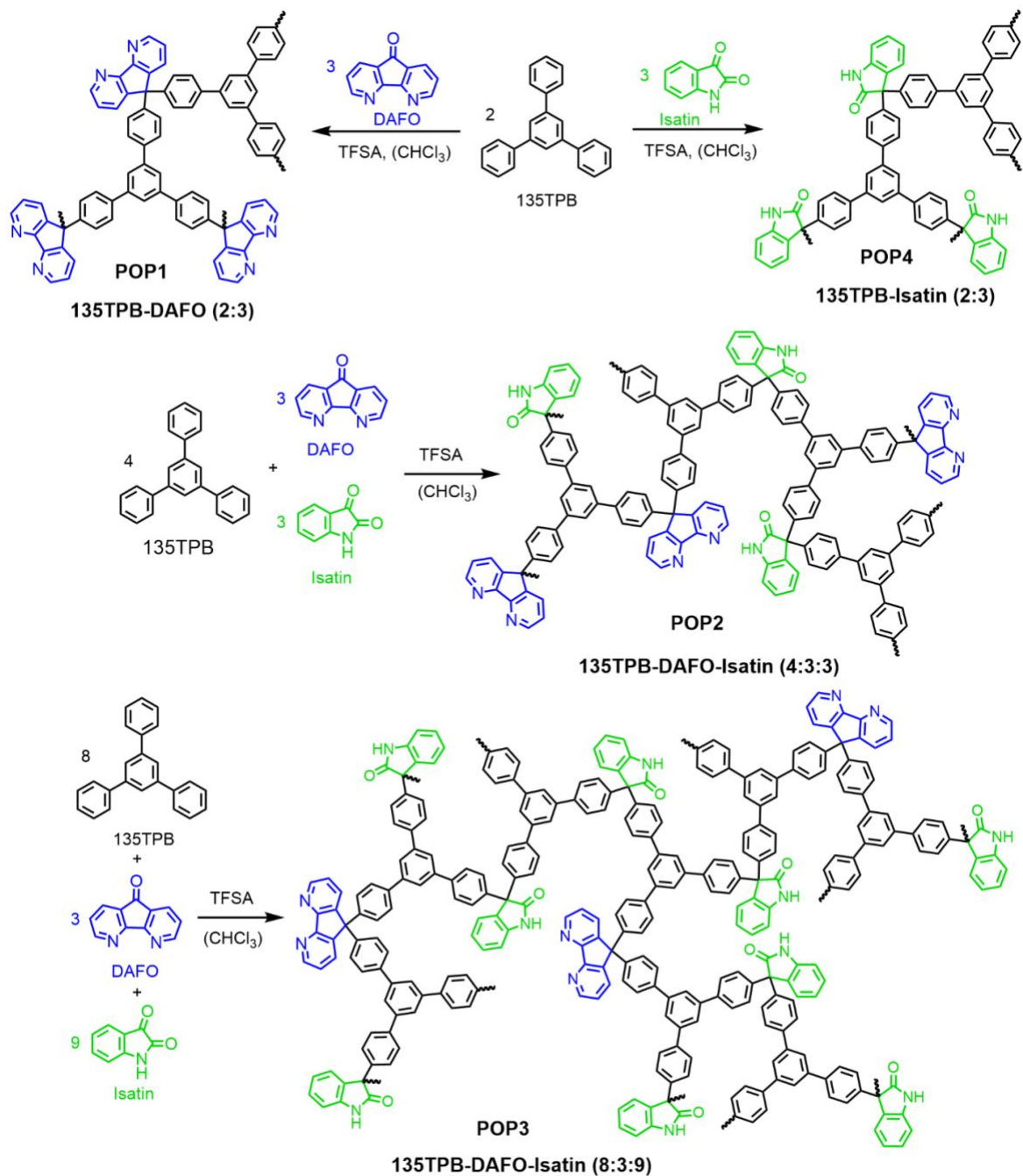
The thermal stability and surface area of these POPs were measured in order to pick out which of them would be employed as catalyst supports. The results of all the POPs obtained with high reaction yields are listed in Table 1. Moreover, the TGA thermograms of POPs, which were dried at 180 ºC for 24 h, are shown in Figures S11-S14. Two losses were observed: a first one associated to the adsorbed water below 200 ºC and a second one related to generalized degradation of material above 400 ºC. The DAFO-containing POPs that were prepared using a TFSA/CHCl$_3$ mixture showed an additional weight loss around 300 ºC, which could be presumably due to occluded solvent within the pores during the reaction.

According to the values summarized in Table 1, the copolymers prepared at 60 ºC and employing CHCl$_3$ as co-solvent exhibited excellent thermal stabilities, above 500 ºC, and the highest S$_{BET}$, superior to 900 m^2/g. Thus, these copolymers were chosen for making the supported Pd(II) catalysts. Hereafter, they will be referred to as SP-POP1, SP-POP2 and SP-POP3.

Table 1. Reaction yield, thermal properties and surface area (S_{BET}) of POPs according to their reaction conditions

POP	Reaction conditions	Reaction yield (%)	Td (ºC)	Char yield at 800 °C (%)	S_{BET} (m^2g^{-1})
POP1-RT	120 h/RT TFSA	92	595	82	805
POP1-60	24 h/RT, 96 h/60 ºC TFSA	93	605	84	785
POP1-60/CHCl₃ **SP-POP1**	24 h/RT, 96 h/60 ºC TFSA/CHCl₃	99	545	82	920
POP2-60	24 h/RT, 96 h/60 ºC TFSA	93	545	82	550
POP2-60/CHCl₃ **SP-POP2**	24 h/RT, 96 h/60 ºC TFSA/CHCl₃	99	525	80	930
POP3-RT/CHCl₃	120 h/RT, TFSA/CHCl₃	99	570	79	820
POP3-60/CHCl₃ **SP-POP3**	24 h/RT, 96 h/60 ºC TFSA/CHCl₃	99	565	81	935
POP4-RT/CHCl₃	120 h/RT TFSA/CHCl₃[a]	99	565	78	760

[a] Reaction conditions previously optimized[45]

3.2. Characterization of catalyst supports

As highly crosslinked materials, all POPs were insoluble in organic solvent, in very low pK$_a$ acids and in high pK$_a$ bases, showing excellent chemical stability. ATR-FTIR and CP/MAS ^{13}C NMR spectra of the SP-POPs selected as catalyst supports were compared with the corresponding

POP4 (135TPB-Isatin) in Figures 1 and 2, respectively. The absorption bands at 1712, 1467 and 1320 cm^{-1} were assigned to the 5-membered lactam rings coming from isatin. The weak C=O stretching band around 1710 cm^{-1} in the spectra of SP-POP1 confirmed the reaction of DAFO. In the case of the copolymers, the band at 1570 cm^{-1}, which was attributed to the C=N stretching from DAFO, was not clearly visible. The CP/MAS ^{13}C NMR spectra confirmed the reaction of the ketones with the aromatic rings; all of them showed a signal at 60 ppm corresponding to the quaternary sp3 carbons. The more characteristic peaks derived from DAFO and isatin moieties are indicated in the spectra. The other signals, between 135-115 ppm, were assigned to aromatic carbons.
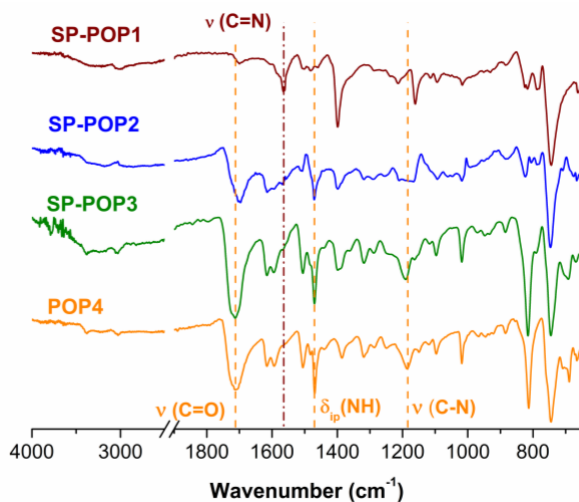
Figure 1. ATR-FTIR spectra of POP-based supports. The POP4 spectrum has been included for comparison sake. The dashed lines indicate the position of the characteristic bands of POPs.
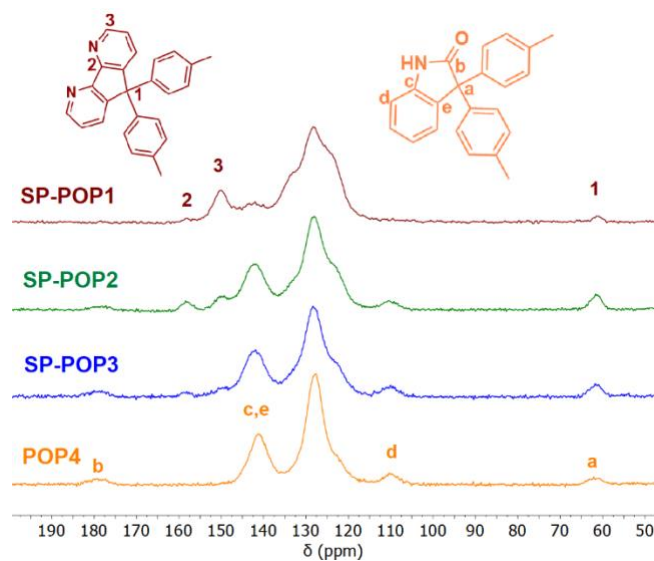
Figure 2. CP/MAS ^{13}C NMR spectra of POP-based supports. The POP4 spectrum has been included for comparison sake.

The amorphous nature of these materials was confirmed by WAXS. The patterns of SP-POPs are compared to that of POP4 in Figure 3. All of them showed similar amorphous halos with three maxima around 14º, 20º and 42º, indicating some regularity in the chains' packing presumably due to the flat and symmetrical triangular shape of the 135TPB. According to according to Bragg's law (λ=2dsenθ, being θ the scattering angle), these maxima corresponded to 0.64, 0.44 and 0.21 nm.
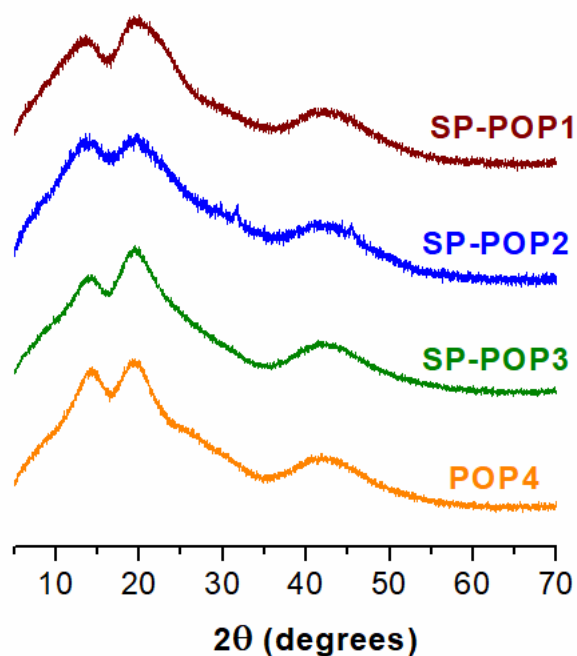
Figure 3. WAXS patterns of POP-based supports. The POP4 pattern has been included for comparison sake.

The surface morphology of the three SP-POPs was explored by FE-SEM. Figure 4 compares the images of these catalyst supports with that of POP4 (135TPB-Isatin). The images of SP-POP1 and SP-POP2, having a higher content of DAFO, revealed very small size particles that form a homogeneous rough surface in which small agglomerates were visible. When the content of isatin was higher, such as in SP-POP3, the surface was rougher due to presence of a higher amount of agglomerates with irregular shapes.
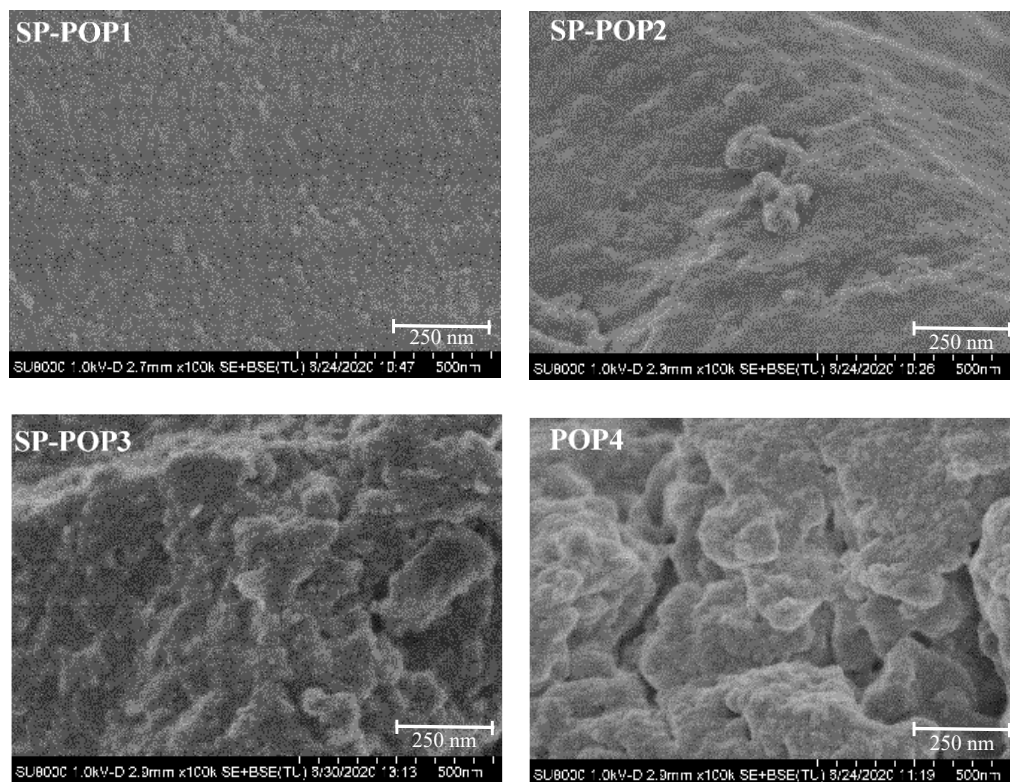
Figure 4. FE-SEM images of SP-POPs. The POP4 image is included for comparison purposes.

The porosity of SP-POPs was studied from the N_2 adsorption/desorption isotherms at -196 ºC, which were compared with that of POP4 in Figure 5(a). As indicated above, prior to measurements, the samples were dried at 250 ºC under vacuum for 10 h. Similar to the behaviour of POP4, the SP-POPs showed a high N_2 uptake at low relative pressures ($P/P_0 < 0.01$), which indicated the presence of micropores.[49] Furthermore, a significant hysteresis was observed in the desorption branch in the whole range of relative pressures, expanding also to the low-pressure region. The low-pressure hysteresis in the nitrogen adsorption isotherms is indicative of the presence of constricted micropore networks (i.e., micropore units are interconnected through narrow pore necks) and it was associated with insufficient equilibrium during the gas adsorption measurements.[50] This finding was more pronounced in sample SP-POP3, and it has already been reported in molecular sieves and chars, as well as it was reported by us for analogous materials

derived from aromatic trifunctional monomers, such as triptycene and 135TPB, and ketones, such as isatin and 2,2,2-trifluoroacetophenone.[45]

Figure 5 (b and c) shows the pore size distributions (PSDs) of the samples; as seen, all three SP-POPs exhibited a marked contribution of the micropores smaller than 1 nm in diameter, with a peak centred at 0.50 nm for SP-POP1 and SP-POP2 and at 0.61 for SP-POP3. In the case of POP4, an additional peak at 0.85 nm was visible. For pores larger than 1 nm in diameter, all samples showed a lower intensity tail, spanning in the range 1-10 nm (see inset in Figure 5(c)).

The main textural parameters and the skeletal density of SP-POPs are summarized in Table 2. The porosity of all three SP-POPs was estimated to be close to 35%; the contribution of the microporosity to the total porosity was around 75% for samples SP-POP1 and SP-POP2, whereas it accounted for ca. 65% for sample SP-POP3. Thus, and according to the pore size distributions of these POPs, the contribution of the mesoporosity due to pore diameters in the 2-10 nm range varied between 25-35%. This corroborated the microporous character of these catalytic supports.
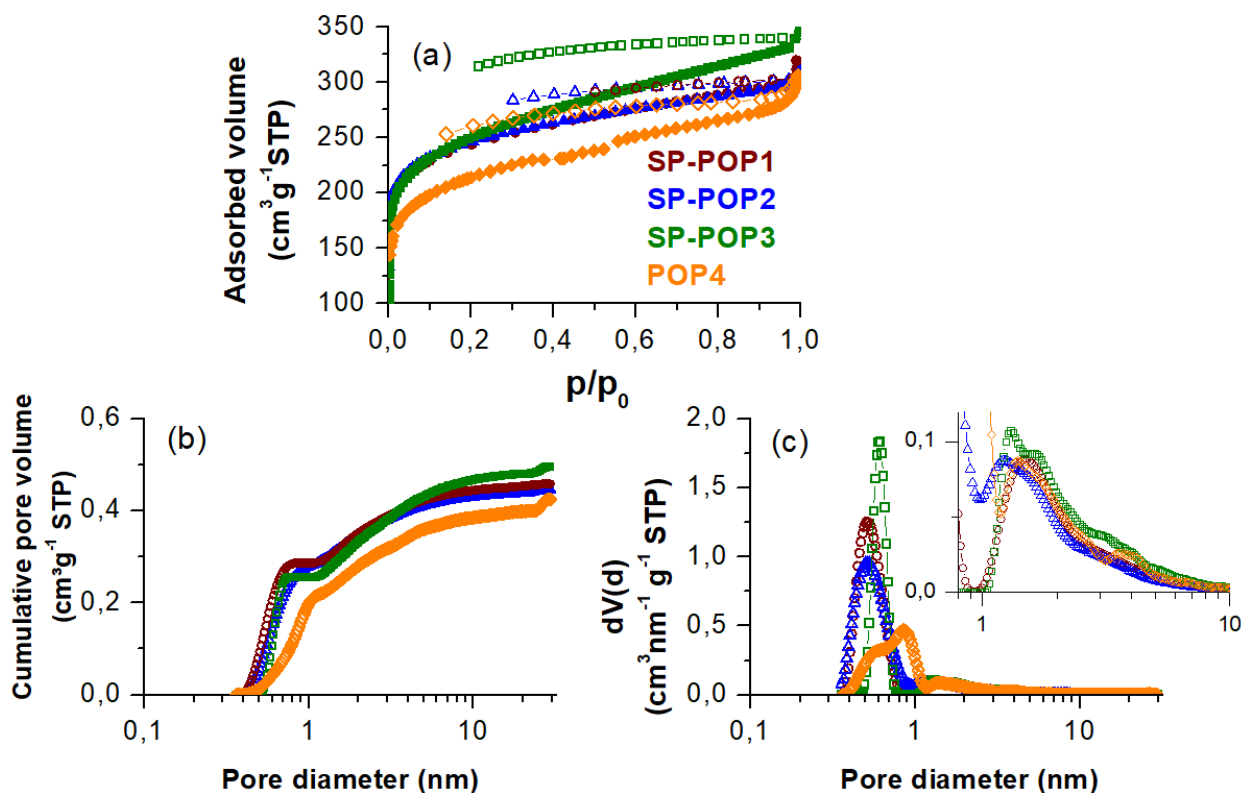
Figure 5. (a) N₂ adsorption (full symbols)/desorption (empty symbols) isotherms measured at -196 ºC, (b) Cumulative pore volume and (c) pore size distribution of the POP-based catalyst supports, as well as that of POP4 for comparison sake.

Table 2. Density and porosity parameters from N₂ adsorption isotherms

SP-POP	density[a]	S_{BET}[b]	V_{total}[c]	V_{micro}[d]	Porosity[e]	Microporosity[f]
SP-POP1	1.044	920	0.47	0.36	33	77
SP-POP2	1.125	930	0.46	0.35	34	76
SP-POP3	0.996	935	0.53	0.34	34	64
POP4	1.145	760	0.43	0.28	33	65

[a] Skeletal density (g cm⁻³) determined by Helium picnometry. [b] Specific surface area (m² g⁻¹) calculated by BET equation. [c] Total pore volume (cm³ g⁻¹) calculated at $P/P_0 = 0.99$. [d] Micropore volume (cm³ g⁻¹), calculated from DR equation. [e] Porosity (%) defined as the V_{total} to (V_{total} + (1/density)) ratio. [f] microporosity (%) defined as the V_{micro}/V_{total} ratio.

3.2. Characterization of Pd-supported catalysts

Palladium(II) coordination reaction of catalyst support was carried out by direct mixing the SP-POP with Pd(OAc)$_2$, as already described in the Experimental section. Hereafter, these materials will be referred to as Pd@SP-POPx, where x is 1, 2 or 3 according to the catalyst support. The ATR-FTIR spectra (Figure 6) showed two peaks at 1700 and 1359 cm^{-1} that were assigned to the acetate groups of the Pd(OAc)$_2$ bipyridine complexes.[51] The asymmetric COO$^-$ stretching band at 1700 cm^{-1} was clearly visible in Pd@SP-POP1 because the catalyst support does not have carbonyl groups in its structure (cf. Figure 1). In the two other supported Pd(II) catalysts, this band overlapped with the C=O band derived from carbonyl group of lactam rings.
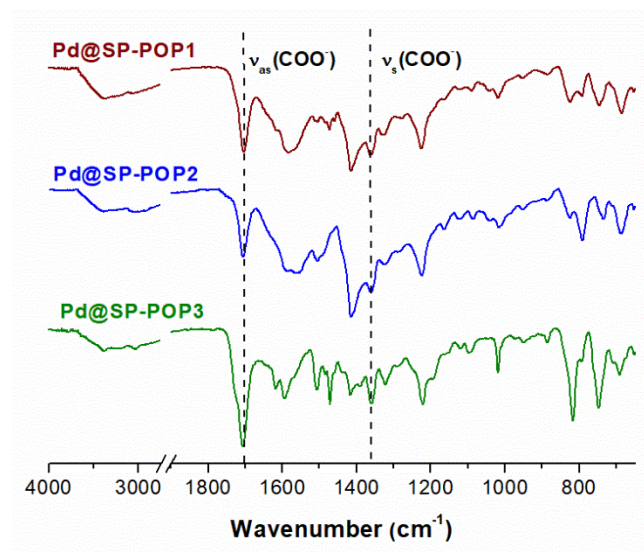

Figure 6. ATR-FTIR spectra of Pd@SP-POPs. The dashed lines indicate the position of the characteristic bands of bridging COO$^-$ groups coming from Pd(OAc)$_2$.

The WAXS patterns of Pd-supported catalysts, depicted in Figure 7, showed very weak reflections around 12° and 33°, which could come from Pd(OAc)$_2$.[52] Comparing the amorphous halos of Pd@SP-POPs with those corresponding to the precursor porous polymers, significant changes in the patterns were observed, especially in the Pd@SP-POP1 and Pd@SP-POP2. In these

cases, the patterns of Pd@SP-POPs showed broader maxima and a lower intensity ratio between them, as compared to those of precursor porous polymers. This finding seems to indicate that the formation of Pd(II) bipyridine complexes mainly led to a higher contribution of small intersegmental distances (high scattering angle side) to the global scattering and, then, a change in the packing of catalyst support could be possible.
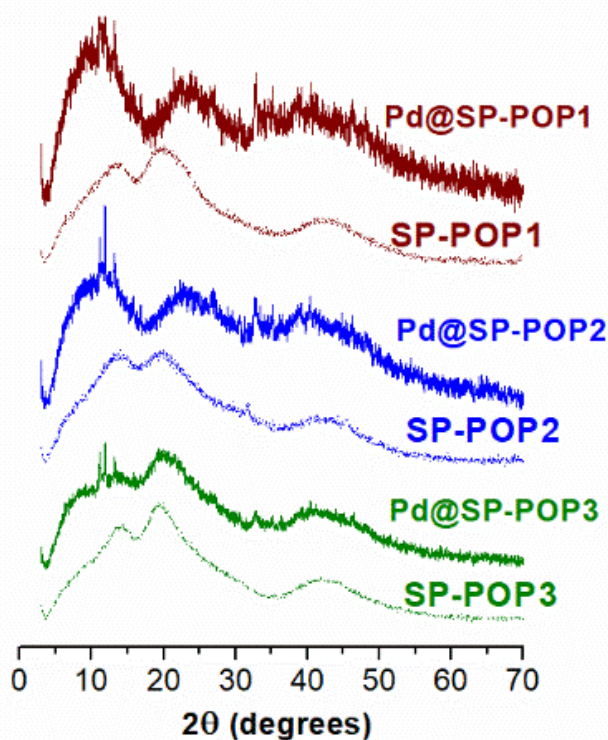

Figure 7. WAXS patterns of Pd@SP-POPs. WAXS patterns of precursor porous polymers (dashed lines) have been included for comparison purposes.

The concentration of Pd in the porous polymer networks was determined by ICP-OES and the values are listed in Table 3. The load amount of Pd embedded in all the SP-POPs was around 95%, related to the theoretical value calculated from their bipyridine content. SEM-EDX metal mapping of the catalysts showed that the palladium content was homogeneously distributed in the catalytic support and XPS analysis of Pd3d binding energies revealed the presence of two intensive doublets

at 337.6 and 342.9 eV, which were related to Pd(II) species. As an example, Figure 8 displays the

SEM-EDX mapping and the XPS spectrum of the Pd@SP-POP2 catalyst. A more detailed and

extensive information about the element mapping of the confined catalyst is showed in the SI

(Section 4).

Table 3. Pd content of POP supported Pd(II) catalysts

Catalyst	Pd content (mg g^{-1})	
	Experimental [a]	Theoretical [b]
Pd@SP-POP1	172	180
Pd@ SP-POP2	111	115
Pd@SP-POP3	64	67

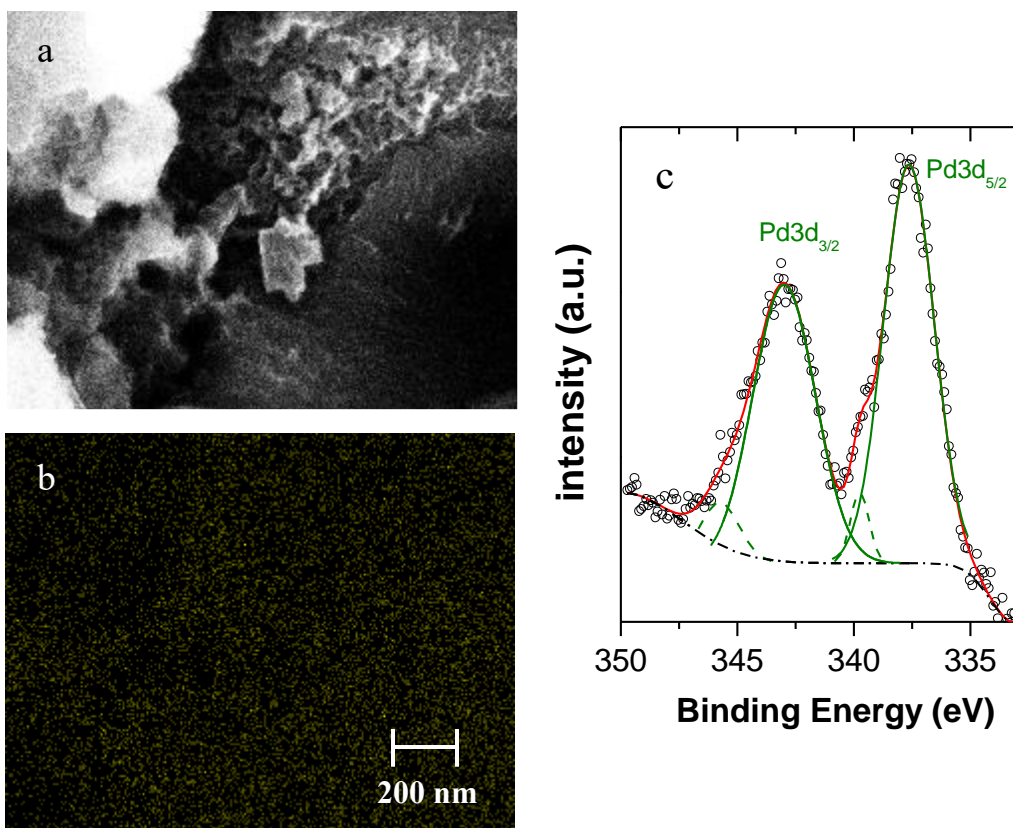[a] Determined by ICP-OES. [b] Calculated from its bipyridine content.

Figure 8. (a) FE-SEM image of Pd@SP-POP2, (b) SEM-EDX mapping and (c) XPS spectrum of the palladium in Pd@SP-POP2.

3.3. Catalytic activity

The Pd@SP-POPs were previously tested in two cross-coupling reaction of 4-bromoanisole and 1,3-dibromo-5-*tert*-butylbenzene with phenylboronic acid, employing classical Suzuki-Miyaura conditions, in order to explore the effect of the DAFO/isatin ratio of the porous polymer on the catalytic activity of catalyst. By these reactions, the number of catalytic conversions (TON) and the frequency of conversions (TOF) of the reaction were determined (Tables S5 and S6). Interestingly, the Pd@SP-POP3, which is the catalyst with the lowest amount of bipyridine units (Pd(OAc)$_2$-binding sites), gave the highest conversion, along with the largest TON and TOF values, for the cross-coupling products (formation of 4-biphenylanisole and 1,3-phenyl-5-*tert*-butylbenzene), when similar reaction conditions and Pd equivalents were employed.[53] For the

formation of 1,3-phenyl-5-*tert*-butylbenzene, it was observed a much higher reaction yield for Pd@SP-POP3 (30% for Pd@SP-POP3 vs yields lower than 5% for the other two catalysts) and TON and TOF values much lower for Pd@SP-POP1 and Pd@SP-POP2 when compared with Pd@SP-POP3. When the amount of Pd was increased to enlarge the reaction yield to values similar to that of Pd@SP-POP3, TON and TOF values augmented, although their values were lower than those observed for Pd@SP-POP3. The highest activity of the Pd@SP-POP3, especially for the bulkiest cross-coupling product, could be related to an enhanced accessibility of reactants to catalytic $Pd(OAc)_2$ sites due to the highest percentage of mesopores in its POP structure.

In view of these findings, we finally chose the Pd@SP-POP2 as the catalytic platform to study the activity of a highly microporous catalyst for Suzuki-Miyaura cross-coupling reaction of aryl halides with phenylboronic acid derivatives. It should be noted that Pd@SP-POP1and Pd@SP-POP2 exhibited similar microporous networks features (cf. Figure 5 and Table 2), comparable thermal stability (Table 1), and alike catalytic behaviour. In addition, the DAFO monomer is much more expensive than isatin, and clearly, Pd@SP-POP2 is economically more competitive than Pd@SP-POP1. Additional, research on this topic is being carried out in order to figure out how the different reactivity of DAFO and isatin could build the framework structure of the polymer. It means to determine whether the core (and consequently the shell) of the porous polymer particle is more or less rich in one monomer than in the other one.

In a first stage, the Suzuki-Miyaura coupling reaction of 4-bromotoluene with phenylboronic acid at 80 ºC, using aerobic conditions, was chosen as a model for optimizing reaction parameters such as the employed solvent and base. Different solvents and bases were tested, as seen in Table 4. Excellent yields of the cross-coupling product were obtained using DMF/H_2O (2/3) and $EtOH/H_2O$ (2/3) mixtures as solvent in presence of bases such as Cs_2CO_3 and Na_2CO_3. According

to these findings and the essential goal of employing green reagents, the EtOH/H_2O (2/3) mixture and the Na_2CO_3 were selected for this study.

Table 4. The optimization of reaction parameters for the Suzuki-Miyaura reaction of 4-bromotoluene with phenylboronic acid[a]
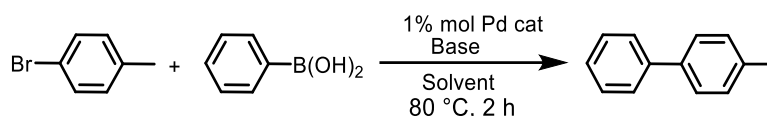
| Entry	Base	Solvent	% Conversion[b]
1	Cs_2CO_3	EtOH/ H_2O (2:3)	94
2	Na_2CO_3	EtOH/ H_2O (2:3)	99
3	Cs_2CO_3	DMF/ H_2O (2:3)	99
4	Na_2CO_3	DMF/ H_2O (2:3)	99
5	Cs_2CO_3	CH_3CN/H_2O (3:1)	61
6	Na_2CO_3	CH_3CN/H_2O (3:1)	53

[a] Reaction conditions: 4-bromotoluene (1 mmol), phenylboronic acid (1.5 mmol), base (2 mmol), Pd@SP-POP2 (1% aryl derivative/catalyst) and solvent (10 mL). [b] Conversion values were obtained by ^{1}H-NMR.

In a second stage, a set of coupling reactions were made, reducing the reaction time and the amount of Pd@SP-POP2, employing other aryl bromides and chlorides with electron-donating groups (*tert*-butyl and OCH_3 groups), as shown in Table 5. In the case of the reaction of 4-bromotoluene in EtOH/H_2O (2/3), the reduction of reaction time to 1 hour (Entry 7) or lessening the amount of Pd-supported catalyst in half (Entry 8) led to lower conversions of reaction than that obtained previously (Entry 6). The reaction of 1-bromo-4-*tert*-butylbenzene with phenylboronic acid for 1 h resulted in 45% conversion (Entry 9), which was much lower than the conversions

obtained for 4-bromotoluene (Entry 7) and 4-bromoanisole (Entry 11) under the same reaction conditions. This finding could be explained under the assumption of a lower diffusion transport of 1-bromo-4-*tert*-butylbenzene through the pores due to the low solubility of the aryl derivative in the solvent mixture. In order to solve this problem, the use of a solvent mixture able to dissolve more efficiently the reagents was considered. Thus, when an EtOH/H_2O volume ratio of 3/2 was used, the conversion of coupling reaction was much higher (97%) (Entry 10). As to the 4-bromoanisole, the complete conversion achieved led us to attempt to change some other reaction parameter from Entry 11: 1) reducing the reaction time to 0.5 h (Entry 12) and 2) and lowering the amount of catalyst at 0.5% mol (Entry 13). None of these changes significantly decreased the reaction yields and the conversions remained higher than 87%.

Aryl chloride derivative, 4-chlorotoluene, was also tested to evaluate the differential catalytic activity of Pd@SP-POP2 in the Suzuki-Miyaura reaction between bromo and chloro substituents. The reaction conversion of 4-chlorotoluene (Entry 14) was moderated (around 70%) as compared with its bromo analogue employing the same conditions (Entry 7). The use of a 3/2 EtOH/H_2O mixture (Entry 15) did not improve the cross-coupling reaction conversion. The products of reaction were determined by GC-MS analysis and the formation of 4,4'-dimethybiphenyl (homocoupling compound formed from 4-chlorotoluene) was observed. This unexpected fact may be interesting to employ this type of catalysts in homocoupling reactions.

Table 5. Suzuki-Miyaura reactions of aryl bromides and chlorides with phenylboronic acid catalyzed by Pd@SP-POP2 catalyst
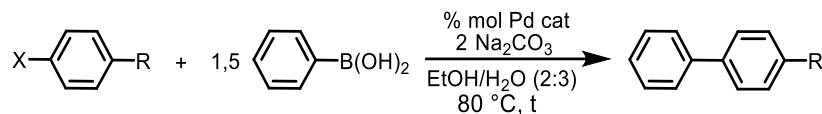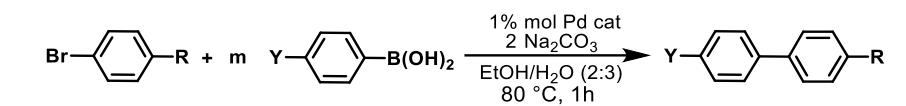

Entry	X	R	Pd cat. (% mol)	Time (h)	Conversion [a] (%)
6	Br	CH_3	1	2	99
7	Br	CH_3	1	1	90
8	Br	CH_3	0.5	2	96
9	Br	^tBu	1	1	45
10[b]	Br	^tBu	1	1	97
11	Br	OCH_3	1	1	100
12	Br	OCH_3	1	0.5	95
13	Br	OCH_3	0.5	1	87
14	Cl	CH_3	1	1	68
15[b]	Cl	CH_3	1	1	71

[a] Conversion values obtained by ^{1}H-NMR. [b] The EtOH/H_2O solvent ratio was 3:2.

In view of the excellent conversions obtained using an excess of 1.5 mol of phenylboronic acid per 1 mol of aryl halide, the ratio of boronic acid/aryl bromide was reduced to 1.2, resulting also in high reactions conversions, as seen in Table 6.

Table 6. Suzuki-Miyaura reactions of aryl bromides with arylboronic acid, varying the ratio between the reagents, catalysed by Pd@SP-POP2 catalyst
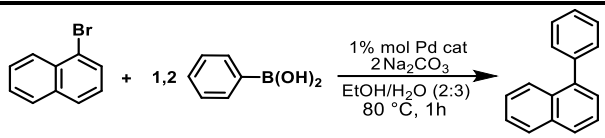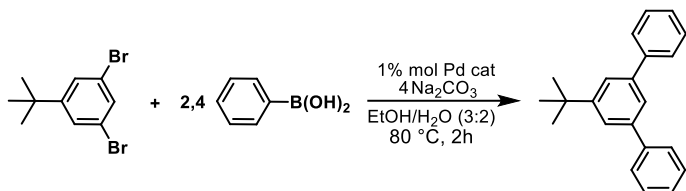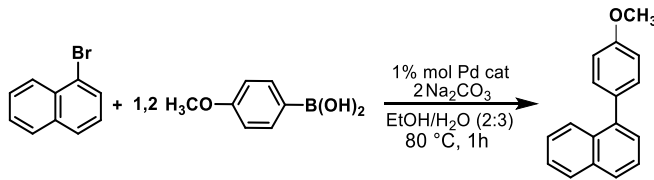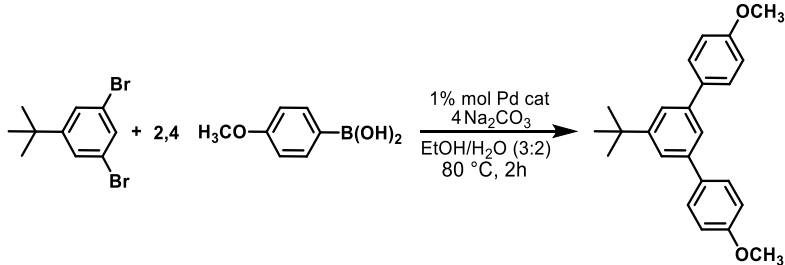

Entry	R	Y	B(OH)$_2$/ArBr ratio	Conversion[a] (%)
7	CH$_3$	H	1.5	90
15	CH$_3$	H	1.2	79
11	OCH$_3$	H	1.5	>99
16	OCH$_3$	H	1.2	>99
10[b]	^{t}Bu	H	1.5	97
17[b]	^{t}Bu	H	1.2	97
18	CH$_3$	OCH$_3$	1.2	99

[a] Conversion values obtained by ^{1}H-NMR. [b] EtOH/H$_2$O solvent ratio was 3:2.

The effectiveness of the heterogeneous catalyst with bulky and difunctional aryl halides and phenylboronic acid and 4-methoxyphenylboronic acid was also tested. The reactions yielded excellent conversions, as seen in Table 7. In particular, Pd@SP-POP2 was able to produce a quantitative yield of the monomer 5'-*tert*-butyl-m-terphenyl (Entry 20). The compound 4-4"-dimethoxy-5'-*tert*-butyl-m-terphenylene, which is precursor of 4-4"-dihydroxy-3,3"-diamino-5'-*tert*-butyl-m-terphenylene (Entry 22), which could be used as a monomer able to produce thermally rearranged materials,[54] was obtained with a yield of 81%. This cross-coupling compound was also prepared by homogeneous catalysis in our laboratory, employing 4% mmol of tetrakis(triphenylphosphine)-palladium(0) as catalyst in a toluene/water 2/3 mixture at 100 ºC for 2 h; the reaction yield was around 75%.

Table 7. Suzuki-Miyaura reactions of bulky reagents catalysed by Pd@SP-POP2

Entry	Reaction	Conversion [a] (%)
19		97
20		99
21		77
22		81

[a] Conversion values obtained by ^{1}H-NMR.

3.4. Scale-up of Suzuki-Miyaura reactions

After the optimization process, scale-up of two Suzuki-Miyaura reactions were carried out by reacting 20-fold the quantity of reagents employed during the catalysis study.

The first scale-up synthesis of 4-methoxy-4'-methylbiphenyl (Entry 18) was made using 1% (0.10 mmol) of Pd@SP-POP2, 50 mmol of 4-bromotoluene, 20 mmol of Na_2CO_3, 60 mmol of acid 4-methoxyphenylboronic and a solvent mixture of 40 mL of EtOH and 60 mL of water. The [1]H-

NMR conversion of the reaction at 80 ºC after 2 h was >99% and the yield of the pure product was of 93%.

The second scale-up synthesis of the precursor monomer, 4-4"-dimethoxy-5'-*tert*-butyl-m-terphenylene (Entry 22), was made by using 1% (0.058 mmol) of Pd@SP-POP2, 6 mmol of 1,3-dibromo-5-*tert*-butylbenzene, 24 mmol of Na_2CO_3, 14 mmol of 4-methoxyphenylboronic acid and a solvent mixture of 35 mL of EtOH and 24 mL of water. Because of the high load of compounds in the reaction batch, a combination of ultrasonic (25% of amplitude) and magnetic stirring was employed. ^{1}H-NMR Conversion of reaction at 80 ºC after 3 h was of 100% and the yield of the pure product was of 96%.

3.5. Catalyst recycling in Suzuki-Miyaura coupling

Recyclability of the heterogeneous catalyst was studied from the Suzuki-Miyaura reaction of 4-bromoanisole with phenylboronic acid (Entry 16). As described in Experimental Section, after each cycle, the catalyst was separated from reaction mixture by centrifugation and washed with EtOH. The first catalytic recycling studies employing 0.5-1% mol of Pd@SP-POP2 were cumbersome, because a loss of the heterogeneous catalyst after each cycle was observed during the catalyst recovery, which could be due to the loss of very small size porous polymer particles (lower than 100-300 nm as was seen by SEM).

It was considered to use magnetic stirring instead of ultrasonic stirring, because the latter is an optimal dispersion method of the particles in suspension but also produces the breaking down of polymer aggregates and, consequently, leads to the formation of smaller size particles, which could easily be lost during the separation and washing of catalyst. Interestingly, the use of magnetic stirring brought about a quantitative conversion for the first cycle (>98%), similar to the value observed when ultrasonic stirring was employed. The conversion was also quantitative for the

second cycle. From the third one, a lessening was observed, which was similar to that found for the fourth one.

Therefore, and because the recycling reactions employed a tiny amount of catalyst, the reaction was scale-up to employ 4% mol of Pd@SP-POP2 catalyst. The results showed that the heterogeneous catalyst retained its catalytic activity after five consecutive cycles; the reaction yield was of 95%, as seen in Figure 9.
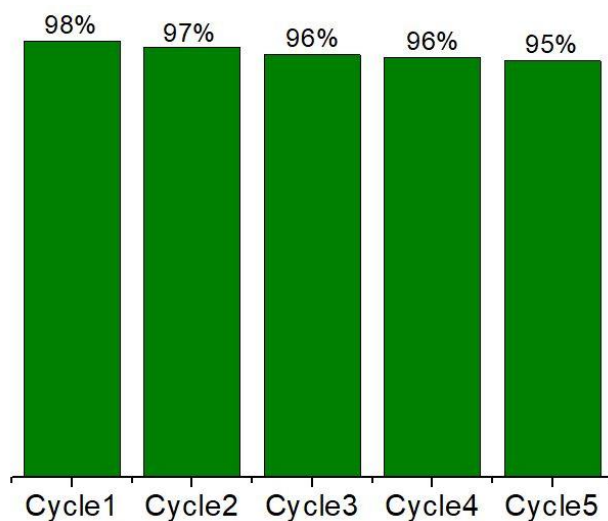

Figure 9. Recyclability of catalyst in the Suzuki–Miyaura reaction. The numbers are the conversion percentage determined by ^{1}H-NMR.

An additional study was made in order to get insight in the recycling process. After each recycling process, the thermal stability of the recovered Pd@SP-POP2 was analyzed by TGA, revealing a weight loss about 5% between 200 and 400 ºC, as seen in Figure S21. This weight loss could be related to the presence of organic compounds (reagents and products) occluded in the pores.

Following this idea, the recycling process was made employing 1% mol of Pd@SP-POP2. After the third cycle, the catalyst was recovered (according to the methodology described for the recycling tests), and washed in hot water at pH 8 and several times with acetone. The initial

reaction was repeated using the dried recovered catalyst and the reaction yield jumped from 63% obtained in the third cycle to 89%. This finding seems to confirm the existence of a clogging of the pores, which blocks the diffusion of the reagents in the subsequent cycles.

Finally, the oxidation states of palladium in the pristine and recovered Pd@SP-POP2 were investigated by XPS analysis of Pd3d binding energies. Comparing the XPS spectra of catalyst before and after reaction, it was observed that Pd(II) was reduced to Pd(0) during the reaction, as seen in Figure S22. On the basis of the peak areas of Pd $3d_{5/2}$ centered at 335.7 eV for Pd(0) and 337.6 eV for Pd(II), the Pd(0)/Pd(II) ratio was calculated to be around 2.2.

4. CONCLUSIONS

New microporous porous organic polymers able to anchor palladium(II)-based catalysts were successfully prepared. Precursor porous organic polymers, POPs, used as catalyst supports were synthesized by a straightforward and high-yield reaction of 1,3,5-triphenylbenzene with ketones activated by electrowithdrawing groups, 4,5-diazafluoren-9-one (DAFO) and 2,3-dioxo-2,3-dihydroindole (isatin), in super acidic media using a TFSA/CHCl$_3$ mixture, in which the strong acid acted as a reaction promoter. These POPs were prepared varying the content of DAFO and isatin in order to modulate the number of bipyridine ligands in the catalyst support. The POPs were characterized employing classical methods of macromolecular chemistry, showing astonishing high thermal stability, well above 475 ºC, and high char yield. These materials were mainly microporous with BET superficial areas superior to 900 m^2 g^{-1}.

The POP-based Pd(II) catalysts were prepared by simple immersion of the POP in a Pd(II) acetate solution. These catalysts gave very high yields for Suzuki-Miyaura reaction, no matter the boronic acid or the aryl derivative employed during the synthesis. The cross-coupling compounds

could be prepared in a green solvent (EtOH/H$_2$O), using low loads of metal, and under aerobic conditions. Moreover, these heterogeneous catalysts could easily be recovered from reaction mixture by washing in EtOH and they could be reused for five consecutive cycles retaining their excellent catalytic activity.

Finally, the synthesis of cross-coupling compounds could easily be scaled-up to give more than 2 g amounts. In particular, it was feasible to make a bulky monomer precursor having a m-terphenylene moiety, with better yields than those obtained by using a common homogeneous Suzuki-Miyaura methodology.

ASSOCIATED CONTENT

Supporting Information

The Supporting Information is available free of charge on the ACS Publications website at DOI.

The Supporting Information includes:

Section 1. Synthesis and characterization of 4,5-diazafluoren-9-one (DAFO)

This section includes the synthesis optimization of the DAFO monomer (Scheme S1, Figure S1 and Figure S2)

Section 2. Synthesis of porous organic polymers. Optimization of reaction conditions

This section includes the synthesis conditions and the characterizations of porous organic polymers (FTIR and CPMAS-NMR) (Table S1, Figures S3 to S10)

Section 3. Thermogravimetric analysis of porous organic polymers

This section includes the thermal characterization of materials (Figures S11 to S14)

Section 4. SEM and SEM-EDX characterization of Pd-supported catalysts

This section includes the results of SEM and SEM-EDX of the three catalytic supports studied (Figures S15 to S20 and Tables S2 to S4)

Section 5. Catalytic activity

This section includes the results about catalytic activity for the three catalysts studied (Table S5 and S6)

Section 6. Catalytic recycling in Suzuki-Miyaura coupling

This section includes thermogravimetric analysis and XPS analysis of the recovered catalyst (Figures S21 and S22).

AUTHOR INFORMATION

Corresponding Authors

*Jesús A. Miguel- *IU CINQUIMA, Univ. de Valladolid, Paseo Belén 5, E-47011 Valladolid, Spain*; orcid.org/0000-0003-2814-5941; *jamiguel@uva.es*

*Cristina Álvarez- *Instituto de Ciencia y Tecnología de Polímeros, ICTP-CSIC, Juan de la Cierva 3, E-28006 Madrid, Spain*; *SMAP, UA-UVA_CSIC, Associated Research Unit to CSIC. Universidad de Valladolid, Facultad de Ciencias, Paseo Belén 7, E-47011 Valladolid, Spain;* orcid.org/0000-0002-5000-0776; *cristina.alvarez@ictp.csic.es*

Authors

Noelia Esteban- *IU CINQUIMA, Univ. de Valladolid, Paseo Belén 5, E-47011 Valladolid, Spain*; orcid.org/0000-0003-2342-6867; isabelnoelia.esteban@alumnos.uva.es

María L. Ferrer- *Materials Science Factory, Instituto de Ciencia de Materiales de Madrid, CMM-CSIC, Campus de Cantoblanco, 28049 Madrid, Spain*; orcid.org/0000-0003-2284-8259; mferrer@icmm.csic.es

Conchi O. Ania- *CEMHTI CNRS (UPR 3079), University of Orléans, 45071 Orléans, France*; orcid.org/0000-0001-9517-8132; conchi.ania@cnrs-orleans.fr

José G. de la Campa- *Instituto de Ciencia y Tecnología de Polímeros, ICTP-CSIC, Juan de la Cierva 3, E-28006 Madrid, Spain*; orcid.org/0000-0003-1882-3104; jcampa@ictp.csic.es

Ángel E. Lozano- *Instituto de Ciencia y Tecnología de Polímeros, ICTP-CSIC, Juan de la Cierva 3, E-28006 Madrid, Spain*; *SMAP, UA-UVA_CSIC, Associated Research Unit to CSIC. Universidad de Valladolid, Facultad de Ciencias, Paseo Belén 7, E-47011 Valladolid, Spain*; *IU CINQUIMA, Univ. de Valladolid, Paseo Belén 5, E-47011 Valladolid*; orcid.org/ 0000-0003-4209-3842; lozano@ictp.csic.es

Author Contributions

The manuscript was written through contributions of all authors. All authors have given approval to the final version of the manuscript.

Noelia Esteban: Investigation, Data processing, Formal analysis, Writing-original draft.

María L. Ferrer: Methodology, Writing-original draft, Validation.

Conchi O. Ania: Investigation, Data processing, Formal analysis, Validation.

José G de la Campa: Methodology, Validation, Formal analysis.

Angel E. Lozano: Conceptualization, Methodology, Validation, Writing-original draft, Funding acquisition, Project administration, Resources, Writing-Reviewing and Editing.

Cristina Álvarez: Investigation, Methodology, Formal analysis, Writing-original draft, Validation, Writing-Reviewing and Editing.

Jesus A. Miguel: Conceptualization, Investigation, Methodology, Validation, Writing-original draft, Funding acquisition, Project administration, Resources, Writing-Reviewing and Editing.

Notes

The authors declare no competing financial interest

REFERENCES

(1)   Beletskaya, I. P.; Alonso, F.; Tyurin, V. The Suzuki-Miyaura Reaction after the Nobel Prize. *Coord. Chem. Rev.* **2019**, *385*, 137–173. https://doi.org/10.1016/j.ccr.2019.01.012.

(2)   Johansson Seechurn, C. C. C.; Kitching, M. O.; Colacot, T. J.; Snieckus, V. Palladium-Catalyzed Cross-Coupling: A Historical Contextual Perspective to the 2010 Nobel Prize. *Angew. Chemie - Int. Ed.* **2012**, *51*, 5062–5085. https://doi.org/10.1002/anie.201107017.

(3)   Seo, T.; Ishiyama, T.; Kubota, K.; Ito, H. Solid-State Suzuki–Miyaura Cross-Coupling Reactions: Olefin-Accelerated C–C Coupling Using Mechanochemistry. *Chem. Sci.* **2019**, *10*, 8202–8210. https://doi.org/10.1039/c9sc02185j.

(4)   Miyaura, N.; Yamada, K.; Suzuki, A. A New Stereospecific Cross-Coupling by the Palladium-Catalyzed Reaction of 1-Alkenylboranes with 1-Alkenyl or 1-Alkynyl Halides. *Tetrahedron Lett.* **1979**, *20*, 3437–3440. https://doi.org/10.1016/S0040-4039(01)95429-2.

(5)   Miyaura, N.; Suzuki, A. Stereoselective Synthesis of Arylated (E) -Alkenes by the Reaction of Alk-1 -Enylboranes with Aryl Halides in the Presence of Palladium Catalyst. *J. Chem. Soc. Chem. Commun.* **1979**, 866–867. https://doi.org/10.1039/C39790000866.

(6)   Kotha, S.; Lahiri, K.; Kashinath, D. Recent Applications of the Suzuki-Miyaura Cross-Coupling Reaction in Organic Synthesis. *Tetrahedron* **2002**, *58*, 9633–9695. https://doi.org/10.1016/S0040-4020(02)01188-2.

(7)   Bankar, D. B.; Hawaldar, R. R.; Arbuj, S. S.; Shinde, S. T.; Gadde, J. R.; Rakshe, D. S.; Amalnerkar, D. P.; Kanade, K. G. Palladium Loaded on ZnO Nanoparticles: Synthesis, Characterization and Application as Heterogeneous Catalyst for Suzuki–Miyaura Cross-Coupling Reactions under Ambient and Ligand-Free Conditions. *Mater. Chem. Phys.* **2020**, *243*, 122561. https://doi.org/10.1016/j.matchemphys.2019.122561.

(8)   Xu, J.; Ou, J.; Chen, L.; Zhang, H.; Ma, S.; Ye, M. Palladium Catalyst Imbedded in

Polymers of Intrinsic Microporosity for the Suzuki–Miyaura Coupling Reaction. *RSC Adv.* **2018**, *8*, 35205–35210. https://doi.org/10.1039/C8RA06214E.

(9)   Suzuki, A. Cross-Coupling Reactions of Organoboranes: An Easy Way to Construct C-C Bonds (Nobel Lecture). *Angew. Chemie - Int. Ed.* **2011**, *50*, 6722–6737. https://doi.org/10.1002/anie.201101379.

(10)   Taheri Kal Koshvandi, A.; Heravi, M. M.; Momeni, T. Current Applications of Suzuki–Miyaura Coupling Reaction in The Total Synthesis of Natural Products: An Update. *Appl. Organomet. Chem.* **2018**, *32*, 1–59. https://doi.org/10.1002/aoc.4210.

(11)   Boström, J.; Brown, D. G.; Young, R. J.; Keserü, G. M. Expanding the Medicinal Chemistry Synthetic Toolbox. *Nat. Rev. Drug Discov.* **2018**, *17*, 709–727. https://doi.org/10.1038/nrd.2018.116.

(12)   Gómez-Martínez, M.; Baeza, A.; Alonso, D. A. Graphene Oxide-Supported Oxime Palladacycles as Efficient Catalysts for the Suzuki–Miyaura Cross-Coupling Reaction of Aryl Bromides at Room Temperature under Aqueous Conditions. *Catalysts* **2017**, *7*, 94. https://doi.org/10.3390/catal7030094.

(13)   Zhang, Y.; Riduan, S. N. Functional Porous Organic Polymers for Heterogeneous Catalysis. *Chem. Soc. Rev.* **2012**, *41*, 2083–2094. https://doi.org/10.1039/c1cs15227k.

(14)   Dong, K.; Sun, Q.; Meng, X.; Xiao, F. S. Strategies for the Design of Porous Polymers as Efficient Heterogeneous Catalysts: From Co-Polymerization to Self-Polymerization. *Catal. Sci. Technol.* **2017**, *7*, 1028–1039. https://doi.org/10.1039/c6cy02458k.

(15)   Paul, S.; Islam, M. M.; Islam, S. M. Suzuki-Miyaura Reaction by Heterogeneously Supported Pd in Water: Recent Studies. *RSC Adv.* **2015**, *5*, 42193–42221. https://doi.org/10.1039/c4ra17308b.

(16)   Huynh, H. V.; Han, Y.; Ho, J. H. H.; Tan, G. K. Palladium(II) Complexes of a Sterically Bulky, Benzannulated N-Heterocyclic Carbene with Unusual Intramolecular C-H⋯Pd and C Carbene⋯Br Interactions and Their Catalytic Activities. *Organometallics* **2006**, *25*, 3267–3274. https://doi.org/10.1021/om060151w.

(17)   Zhang, F.; Liang, C.; Wu, X.; Li, H. A Nanospherical Ordered Mesoporous Lewis Acid Polymer for the Direct Glycosylation of Unprotected and Unactivated Sugars in Water. *Angew. Chemie - Int. Ed.* **2014**, *53*, 8498–8502. https://doi.org/10.1002/anie.201404353.

(18)   Lu, S.; Hu, Y.; Wan, S.; McCaffrey, R.; Jin, Y.; Gu, H.; Zhang, W. Synthesis of Ultrafine and Highly Dispersed Metal Nanoparticles Confined in a Thioether-Containing Covalent Organic Framework and Their Catalytic Applications. *J. Am. Chem. Soc.* **2017**, *139*, 17082–17088. https://doi.org/10.1021/jacs.7b07918.

(19)   Wei, Y.; Mao, Z.; Li, Z.; Zhang, F.; Li, H. Aerosol-Assisted Rapid Fabrication of a Heterogeneous Organopalladium Catalyst with Hierarchical Bimodal Pores. *ACS Appl. Mater. Interfaces* **2018**, *10*, 13914–13923. https://doi.org/10.1021/acsami.8b04543.

(20)   Wang, K.; Liu, J.; Zhang, F.; Zhang, Q.; Jiang, H.; Tong, M.; Xiao, Y.; Son Phan, N. T.; Zhang, F. Primary Amine-Functionalized Mesoporous Phenolic Resin-Supported Palladium Nanoparticles as an Effective and Stable Catalyst for Water-Medium Suzuki-Miyaura Coupling Reactions. *ACS Appl. Mater. Interfaces* **2019**, *11*, 41238–41244.

https://doi.org/10.1021/acsami.9b11459.

(21)   Kostas, I. D.; Tenchiu, A. C.; Arbez-Gindre, C.; Psycharis, V.; Raptopoulou, C. P. Room-Temperature Suzuki-Miyaura Coupling of Aryl Bromides with Phenylboronic Acid Catalyzed by a Palladium Complex with an Inexpensive Nitrogen-Containing Bis(Phosphinite) Ligand. *Catal. Commun.* **2014**, *51*, 15–18. https://doi.org/10.1016/j.catcom.2014.03.014.

(22)   Das, P.; Linert, W. Schiff Base-Derived Homogeneous and Heterogeneous Palladium Catalysts for the Suzuki-Miyaura Reaction. *Coord. Chem. Rev.* **2016**, *311*, 1–23. https://doi.org/10.1016/j.ccr.2015.11.010.

(23)   Ding, S. Y.; Gao, J.; Wang, Q.; Zhang, Y.; Song, W. G.; Su, C. Y.; Wang, W. Construction of Covalent Organic Framework for Catalysis: Pd/COF-LZU1 in Suzuki-Miyaura Coupling Reaction. *J. Am. Chem. Soc.* **2011**, *133*, 19816–19822. https://doi.org/10.1021/ja206846p.

(24)   Jaworski, J. N.; Kozack, C. V.; Tereniak, S. J.; Knapp, S. M. M.; Landis, C. R.; Miller, J. T.; Stahl, S. S. Operando Spectroscopic and Kinetic Characterization of Aerobic Allylic C-H Acetoxylation Catalyzed by Pd(OAc)2/4,5-Diazafluoren-9-One. *J. Am. Chem. Soc.* **2019**, *141*, 10462–10474. https://doi.org/10.1021/jacs.9b04699.

(25)   Chen, X.; Zhu, H.; Wang, W.; Du, H.; Wang, T.; Yan, L.; Hu, X.; Ding, Y. Multifunctional Single-Site Catalysts for Alkoxycarbonylation of Terminal Alkynes. *ChemSusChem* **2016**, *9*, 2451–2459. https://doi.org/10.1002/cssc.201600660.

(26)   Wang, H.; Yuan, H.; Wang, X.; Zhao, J.; Wei, D.; Shi, F. Synthesis of Amides-Functionalized POPs-Supported Nano-Pd Catalysts for Phosphine Ligand-Free

Heterogeneous Hydroaminocarbonylation of Alkynes. *Adv. Synth. Catal.* **2020**, *362*, 2348–2353. https://doi.org/10.1002/adsc.202000242.

(27)   Kim, S.; Kim, B.; Dogan, N. A.; Yavuz, C. T. Sustainable Porous Polymer Catalyst for Size-Selective Cross-Coupling Reactions. *ACS Sustain. Chem. Eng.* **2019**, *7*, 10865–10872. https://doi.org/10.1021/acssuschemeng.9b01729.

(28)   Du, Z. L.; Dang, Q. Q.; Zhang, X. M. Heptazine-Based Porous Framework Supported Palladium Nanoparticles for Green Suzuki-Miyaura Reaction. *Ind. Eng. Chem. Res.* **2017**, *56*, 4275–4280. https://doi.org/10.1021/acs.iecr.6b05039.

(29)   Qian, Y.; Jeong, S. Y.; Baeck, S. H.; Jin, M. J.; Shim, S. E. A Palladium Complex Confined in a Thiadiazole-Functionalized Porous Conjugated Polymer for the Suzuki-Miyaura Coupling Reaction. *RSC Adv.* **2019**, *9*, 33563–33571. https://doi.org/10.1039/c9ra06709d.

(30)   Xu, W.; Liu, C.; Xiang, D.; Luo, Q.; Shu, Y.; Lin, H.; Hu, Y.; Zhang, Z.; Ouyang, Y. Palladium Catalyst Immobilized on Functionalized Microporous Organic Polymers for C-C Coupling Reactions. *RSC Adv.* **2019**, *9*, 34595–34600. https://doi.org/10.1039/c9ra07303e.

(31)   Zhu, G.; Ren, H. *Porous Organic Frameworks*; SpringerBriefs in Molecular Science; Springer Berlin Heidelberg: Berlin, Heidelberg, 2015. https://doi.org/10.1007/978-3-662-45456-5.

(32)   Li, B.; Guan, Z.; Wang, W.; Yang, X.; Hu, J.; Tan, B.; Li, T. Highly Dispersed Pd Catalyst Locked in Knitting Aryl Network Polymers for Suzuki-Miyaura Coupling Reactions of Aryl Chlorides in Aqueous Media. *Adv. Mater.* **2012**, *24*, 3390–3395.

https://doi.org/10.1002/adma.201200804.

(33)   Bhanja, P.; Modak, A.; Bhaumik, A. Porous Organic Polymers for CO2 Storage and Conversion Reactions. *ChemCatChem* **2018**, *10*, 1–15. https://doi.org/10.1002/cctc.201801046.

(34)   Kaur, P.; Hupp, J. T.; Nguyen, S. T. Porous Organic Polymers in Catalysis: Opportunities and Challenges. *ACS Catal.* **2011**, *1* (7), 819–835. https://doi.org/10.1021/cs200131g.

(35)   Das, S.; Heasman, P.; Ben, T.; Qiu, S. Porous Organic Materials: Strategic Design and Structure-Function Correlation. *Chem. Rev.* **2017**, *117*, 1515–1563. https://doi.org/10.1021/acs.chemrev.6b00439.

(36)   Aguilar-Lugo, C.; Suárez-García, F.; Hernández, A.; Miguel, J. A.; Lozano, Á. E.; De La Campa, J. G.; Álvarez, C. New Materials for Gas Separation Applications: Mixed Matrix Membranes Made from Linear Polyimides and Porous Polymer Networks Having Lactam Groups. *Ind. Eng. Chem. Res.* **2019**, *58*, 9585–9595. https://doi.org/10.1021/acs.iecr.9b01402.

(37)   Olah, G. A.; Germain, A.; Lin, H. C.; Forsyth, D. A. Electrophilic Reactions at Single Bonds. XVIII. Indication of Protosolvated de Facto Substituting Agents in the Reactions of Alkanes with Acetylium and Nitronium Ions in Superacidic Media. *J. Am. Chem. Soc.* **1975**, *97*, 2928–2929. https://doi.org/10.1021/ja00843a067.

(38)   Olah, G. A. Superelectrophiles. *Angew. Chemie Int. Ed. English* **1993**, *32*, 767–788. https://doi.org/10.1002/anie.199307673.

(39) Olah, G. A.; Klumpp, D. A. Superelectrophilic Solvation. *Acc. Chem. Res.* **2004**, *37*, 211–220. https://doi.org/10.1021/ar020102p.

(40) Olah, G. A.; Klumpp, D. A. *Superelectrophiles and Their Chemistry*; Wiley, J., Sons, I., Eds.; John Wiley & Sons, Inc.: Hoboken, NJ, USA, New Jersey, 2007. https://doi.org/10.1002/9780470185124.

(41) Pulido, B. A.; Waldron, C.; Zolotukhin, M. G.; Nunes, S. P. Porous Polymeric Membranes with Thermal and Solvent Resistance. *J. Memb. Sci.* **2017**, *539*, 187–196. https://doi.org/10.1016/j.memsci.2017.05.070.

(42) Hernandez, M. C. G.; Zolotukhin, M. G.; Fomine, S.; Cedillo, G.; Morales, S. L.; Fröhlich, N.; Preis, E.; Scherf, U.; Salmón, M.; Chávez, M. I.; Cárdenas, J.; Ruiz-Trevino, A. Novel, Metal-Free, Superacid-Catalyzed "Click" Reactions of Isatins with Linear, Nonactivated, Multiring Aromatic Hydrocarbons. *Macromolecules* **2010**, *43*, 6968–6979. https://doi.org/10.1021/ma101048z.

(43) Olvera, L. I.; Ruiz-Treviño, F. A.; Balmaseda, J.; Ronova, I. A.; Zolotukhin, M. G.; Carreón-Castro, M. P.; Lima, E.; Cárdenas, J.; Gaviño, R. Microporous Polymers from Superacid Catalyzed Polymerizations of Fluoroketones with P-Quaterphenyl: Synthesis, Characterization, and Gas Sorption Properties. *Polymer (Guildf).* **2016**, *102*, 221–230. https://doi.org/10.1016/j.polymer.2016.09.021.

(44) Zolotukhin, M. G.; Colquhoun, H. M.; Zolotukhin, M. G.; Khalilov, L. M.; Dzhemilev, U. M. Superelectrophiles in Aromatic Polymer Chemistry. *Macromolecules* **2001**, *34*, 1122–1124. https://doi.org/10.1021/ma001579o.

(45)   Lopez-Iglesias, B.; Suárez-García, F.; Aguilar-Lugo, C.; González Ortega, A.; Bartolomé, C.; Martínez-Ilarduya, J. M.; De La Campa, J. G.; Lozano, Á. E.; Álvarez, C. Microporous Polymer Networks for Carbon Capture Applications. *ACS Appl. Mater. Interfaces* **2018**, *10*, 26195–26205. https://doi.org/10.1021/acsami.8b05854.

(46)   Inglett, G. E.; Frederick Smith, G. The Formation of a New Nitrogen Heterocyclic Ring System by the Loss of Carbon Monoxide from 1,10-Phenanthroline-5,6-Quinone. *J. Am. Chem. Soc.* **1950**, *72*, 842–844. https://doi.org/10.1021/ja01158a051.

(47)   Zhao, J. F.; Chen, L.; Sun, P. J.; Hou, X. Y.; Zhao, X. H.; Li, W. J.; Xie, L. H.; Qian, Y.; Shi, N. E.; Lai, W. Y.; Fan, Q. L.; Huang, W. One-Pot Synthesis of 2-Bromo-4,5-Diazafluoren-9-One via a Tandem Oxidation-Bromination-Rearrangement of Phenanthroline and Its Hammer-Shaped Donor-Acceptor Organic Semiconductors. *Tetrahedron* **2011**, *67*, 1977–1982. https://doi.org/10.1016/j.tet.2010.12.065.

(48)   Jagiello, J.; Olivier, J. P. 2D-NLDFT Adsorption Models for Carbon Slit-Shaped Pores with Surface Energetical Heterogeneity and Geometrical Corrugation. *Carbon N. Y.* **2013**, *55*, 70–80. https://doi.org/10.1016/j.carbon.2012.12.011.

(49)   Thommes, M.; Kaneko, K.; Neimark, A. V; Olivier, J. P.; Rodriguez-reinoso, F.; Rouquerol, J.; Sing, K. S. W. Physisorption of Gases, with Special Reference to the Evaluation of Surface Area and Pore Size Distribution (IUPAC Technical Report). **2015**, *87*, 1051–1069. https://doi.org/10.1515/pac-2014-1117.

(50)   Silvestre-Albero, A. M.; Juárez-Galán, J. M.; Silvestre-Albero, J.; Rodríguez-Reinoso, F. Low-Pressure Hysteresis in Adsorption: An Artifact? *J. Phys. Chem. C* **2012**, *116*, 16652–

16655. https://doi.org/10.1021/jp305358y.

(51)   Stoyanov, E. S. IR Study of the Structure of Palladium(II) Acetate in Chloroform, Acetic

Acid, and Their Mixtures in Solution and in Liquid-Solid Subsurface Layers. *J. Struct.*

Chem. **2000**, *41*, 440–445. https://doi.org/10.1007/BF02742003.

(52)   Kirik, S. D.; Mulagaleev, R. F.; Blokhin, A. I. [Pd(CH3COO)2]n from X-Ray Powder

Diffraction Data. *Acta Crystallogr. Sect. C Cryst. Struct. Commun.* **2004**, *60*, m449–m450.

https://doi.org/10.1107/S0108270104016129.

(53)   Yılmaz Baran, N.; Baran, T.; Menteş, A. Production of Novel Palladium Nanocatalyst

Stabilized with Sustainable Chitosan/Cellulose Composite and Its Catalytic Performance in

Suzuki-Miyaura Coupling Reactions. *Carbohydr. Polym.* **2018**, *181*, 596–604.

https://doi.org/10.1016/j.carbpol.2017.11.107.

(54)   Kim, S.; Lee, Y. M. Rigid and Microporous Polymers for Gas Separation Membranes. *Prog.*

Polym. Sci. **2015**, *43*, 1–32. https://doi.org/10.1016/j.progpolymsci.2014.10.005.

Table of Contents